Analytical Study of Radiative Mixed Convection Flow of Micropolar Nanofluid over an Exponentially Permeable Stretching Sheet with Internal Heat Generation

Eltayeb Awad[1] , Yaseen Abbaker[2], Amal Rahamtalla[3], & Fakhraldeen Gamar[4]

[1]*Department of Mathematics, University of El Imam El Mahdi Kosti, White Nile State, Sudan,*
Email: Eltayebawad333@gmail.com
[2,3]*Department of Mathematics Holy Quran University and Tassel of Science, Wad Madani, Sudan.*
Email:yaseenabbaker@gmail.com
Email:amellabass123@gmail.com
[4]*Department of Mathematics, University of El Geneina, El-Geneina-61115, West Darfur, Sudan*
Email: gamarkhater1994@gmail.com

Abstract:

The growing demand for increased heat conduction in thermal science-based fluids for better industrial performance and engineering applications has sparked substantial interest. This study looks at how internal heat generation affects the mixed convection flow of a micro polar nano fluid over an exponentially stretched plate, taking into account the Brownian motion parameter and the Prandtl number. The semi-analytical Galerkin weighted residual approach is used to solve a nonlinear ordinary differential equations (ODE) system. The Galerkin technique is used iteratively to evaluate various parameter values, with all computations carried out in the Maple software environment for accuracy. Graphical representations reveal how critical parameters influence the temperature, velocity, concentration, and motion fields within the boundary layer. The Sherwood and Nusselt numbers, as well as the local skin friction coefficients, are tabulated. The findings are validated and highlighted as significant by comparing them to current literature.

Keywords: Radiative Mixed, Convection Flow, Micro polar Nano fluid, Exponentially, Permeable Stretching Sheet.

Introduction

Nano fluids are a type of complicated fluid made by distributing nanoparticles, or particles smaller than a nanometer, into more common base fluids like oils, ethylene glycol, or water, nanoparticles, such as metals, metal oxides, carbides, or carbon-based compounds, considerably improve the thermal and physical properties of base fluids. Because of this advancement, nan fluids are particularly beneficial in applications requiring improved fluid performance and efficient heat transfer. Choi [1] proposed using nanoparticles to increase the thermal conductivity and heat transfer capabilities of traditional heat transfer fluids, this revolutionary technology effectively eliminated the usage of bigger particles, which usually caused sedimentation and blockage in heat transfer systems. Ganga, and his team [2] scrutinized the MHD Buongiorno nan fluid flowing on a vertical surface with the heat source. Likewise, Hakeem et.al [3].Reported analytical and numerical Analysis of the hydro magnetic flow of Nano fluids using the Buongiorno model on a vertical plate. Moreover, Hakeem and his associates [4] performed the effect of inclined Lorentz forces on entropy generation in viscoelastic fluid flow over a stretching sheet under nonlinear thermal radiation and heat source/sink. Furthermore, Khan et al. [5] Addressed the MHD flow of third-grade fluid through a vertical micro-channel filled with porous zone using a semi-implicit finite difference scheme In addition, Hasin et al [6] analyzed the effect of nanoparticles on vegetable oil as a cutting fluid through fractional ramped analysis. Additionally, Khan et al [7]. Managed a time-fractional model of Maxwell nan fluid flow through a channel with applications in grease dynamics, Besides, The effect of partial slip boundary conditions on the flow and heat transfer of nan fluids via a stretching sheet with a constant wall temperature was investigated by, Noghrehabadi et al [8].also, Khan and, Pop [9].investigated boundary layer flow of a nan fluid past stretching plate. As well, Nadeem et al [10]. Proposed numerical treatment of boundary layer flow and heat transfer of Oldroyd-B nan fluid along a stretching surface, What's more, Makinde

et al [111investigated the buoyancy effects on MHD stagnation point flow and heat transmission of nan fluid through a convectively heated stretching/shrinking sheet.

Nano fluids, a class of fluids engineered by dispersing nanoparticles into conventional base fluids, have garnered great interest due to their superior thermal and flow qualities. These fluids are noted for their high thermal conductivity and heat transfer capability, making them perfect for a variety of applications such as heat exchangers, cooling systems, and lubrication operations. When coupled with the unique characteristics of micro polar fluids, which exhibit microstructure effects such as particle rotations and non-Newtonian behavior, the resulting micro polar nan fluids provide further improvements in fluid dynamics and heat transfer efficiency.

Micro polar fluids differ from classical Newtonian fluids by exhibiting complex flow features, including the presence of spin and angular momentum within the fluid's microstructure. These properties lead to a unique set of behavior under different flow conditions, especially when coupled with the enhanced thermal properties of Nano fluids. In many industrial and engineering applications, it is important to model fluid flows over surfaces with varying temperature profiles, such as those found in systems with exponentially preamble sheets. Eringen [12, 13] investigated and developed micro polar fluid. Numerous review articles discussing the theory and its applications were presented by Ariman et al. [14, 15], further, in the previous decades, Advancements were established by Lukaszewicz [16] and Eringen [17]. Recently, Oreyeni et al. [18] proposed triple stratification influence on an inclined hydromagnetic bioconvective flow of micro polar nan fluid in the presence of exponential space and heat source Koriko et al. [19] investigated the weak and strong solute transfer levels of the hydromantic micro polar fluid containing nanoparticles and gyrotactic organisms. Koriko et al. [20] conducted the joint impact of nonlinear thermal radiation and stratification on the boundary layer flow of micro polar fluid. Ahmadi [21] investigated the behavior of an incompressible micro polar boundary layer flowing on a semi-infinite sheet. Khine [22] presented the spin-vorticity relation for unidirectional plane flows of micro polar fluids. In addition, Peddieson and Nitt [23] studied the steady stagnation point behavior of the micro polar boundary layer theory.

The exponential preamble sheet, with its temperature variation increasing exponentially along its surface, introduces significant challenges to understanding the thermal boundary layer and heat transport features. The interaction of the micro polar nan fluid with such a surface can cause complex flow and heat transfer phenomena, which are influenced by both the fluid's non-Newtonian properties and the changeable surface temperature. Mazhar et al [24] controlled radiative mixed convection of Casson nanofluid across an increasingly permeable stretched sheet to generate internal heat additionally, Ibukun et al [25], investigated unsteady Casson Nanofluid flow on a stretched surface with the help of energy transmission, convective and slip boundary conditions, and Buongiorno [26] revealed transport in nan fluids. Likewise, Noghrehabadi et al [27], meanwhile, Khan, and Pop, [28].Moreover, the study of heat transfer towards stretching plate at stagnation flow has been proposed by numerous scientists such as Nadeem, et al [29], Makinde, and his teams [30], and, Haroun, and his associates [31]

Ohaegbue, et al [32] they have investigated the theoretical Relevance of thermal criticality and a two-step exothermic reaction on Casson-Williamson fluid dynamics behavior through a fixed vertical channel. Furthermore, Maxwell stagnation points fluid with radiation and hyperbolic nonlinear porosity flow with Riga plate and Arrhenius reaction discussed by Salawu, et al [33, 34].

This research investigates the radiative mixed convection flow of a micropolar nanofluid via an increasingly permeable stretched sheet with internal heat generation. The governing partial differential equations (PDEs) are transformed into nonlinear ordinary differential equations (ODEs) by similarity transformations. The ODEs are then solved using a semi-analytical approach, specifically the Galerkin weighted residual scheme. The importance of this study arises from its addition to our understanding of heat transmission and flow dynamics in systems involving micro polar nan fluids, radiation, and internal heat generation. The findings have important implications for improving the design and efficiency of engineering systems that encounter such scenarios.

Mathematical Statement of the problem

Figure 1 depicts the geometry and flow characteristics of a time-independent, incompressible, two-dimensional viscous flow of micro solar nan fluid. Beginning at x=y=0, a fixed point in the xz plane, the permeable sheet expands vertically exponentially. This surface stretching generates motion in the incompressible non-Newtonian fluid. Natural convection takes place inside the fluid when changes in temperature lead to variations in density, which in turn induces buoyant forces to act on the fluid particles. The flow is parallel to the x-axis at the surface. As seen in the picture, a magnetic field B_0 is applied perpendicular to the direction of flow. Given the supplied magnetic field, the induced magnetic field is considered negligible because the pressure [19.21, 24, and 37]

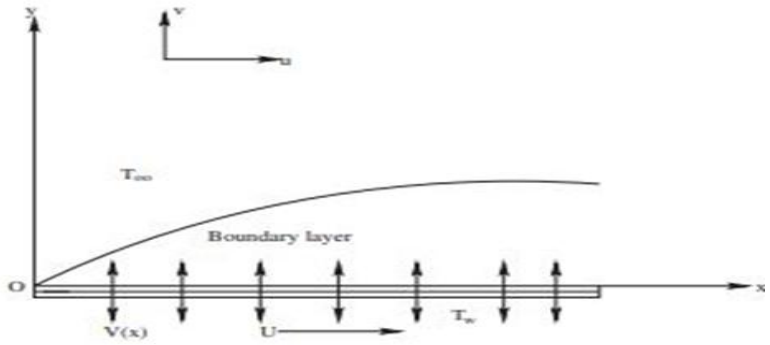

Fig .1 Graphical depiction of the flow

$$\frac{\partial u}{\partial x}+\frac{\partial v}{\partial y}=0, \tag{1}$$

$$u\frac{\partial u}{\partial x}+v\frac{\partial u}{\partial y}=\left(\frac{\mu+k}{\rho}\right)\left(\frac{\partial^2 u}{\partial y^2}\right)+\left(\frac{k}{\rho}\right)\frac{\partial N}{\partial y}-\left(\frac{\sigma B^2{}_0}{\rho_f}+\frac{\nu}{k_1}\right)u+g[\beta^{+}(T-T_\infty)+\beta^{-}(C-C_\infty)], \tag{2}$$

$$\rho_j\left[u\frac{\partial N}{\partial x}+v\frac{\partial N}{\partial y}\right]=\gamma\frac{\partial^2 N}{\partial y^2}-k\left[2N+\frac{\partial u}{\partial y}\right], \tag{3}$$

$$\left(u\frac{\partial T}{\partial x}+v\frac{\partial T}{\partial y}\right)=\alpha\left(\frac{\partial^2 T}{\partial y^2}\right)+\tau\left(D_B\frac{\partial C}{\partial y}\frac{\partial T}{\partial y}\right)+\tau\frac{D_T}{T_\infty}\left(\frac{\partial T}{\partial y}\right)^2-\frac{1}{\rho C_P}\frac{\partial q_r}{\partial y}+\frac{Q}{(\rho C_P)_f}(T-T_\infty), \tag{4}$$

$$u\frac{\partial C}{\partial x}+v\frac{\partial C}{\partial y}=D_B\frac{\partial^2 C}{\partial y^2}+\frac{D_T}{T_\infty}\frac{\partial^2 T}{\partial y^2}-k^{*}(C-C_\infty), \tag{5}$$

Boundary conditions are:

$$\left.\begin{aligned} &u=U_w,\quad v=-V(x)\,,\ N=-n\,\frac{\partial u}{\partial y}\,,T=T_w,\quad D_B\frac{\partial C}{\partial y}+\frac{D_T}{T_\infty}\frac{\partial T}{\partial y}=0,\ at\ y=0,\\ &u\to 0\,,\qquad N\to 0,\ T\to T_\infty,\qquad C\to C_\infty\ as\ y\to\infty. \end{aligned}\right] \tag{6}$$

Where u, v, and w are velocity components along x- and y- directions T and C are the temperature and concentration of the fluid respectively, μ is viscosity, K is vortex viscosity, ρ is the density, N is the microrotation velocity, γ is velocity slip parameter, j is the density of micro-inertia, fluid, v is the kinematic viscosity D_B Is the Brownian motion diffusion coefficient, k^{*} Is the dimensionless chemical reaction parameter, D_T Is the thermo phreatic diffusion coefficient, σ is the electrical conductivity of the fluid, B_0 is a uniform magnetic field along the y-axis C_p is the specific heat constant pressure, T_∞ Is ambient temperature C_∞ Is ambient concentrations.

The similarity variables

$$\left.\begin{aligned} &\eta=y\sqrt{\frac{U_0}{2\nu L}}e^{\frac{x}{2L}},u=U_0e^{\frac{x}{L}}f'(\eta),\ \ v=-\sqrt{\frac{\nu\,U_0}{2L}}e^{\frac{x}{2L}}\big(f(\eta)+\eta f'(\eta)\big),\\ &N=\sqrt{\frac{U_0}{2\nu L}}U_0\,e^{\frac{3x}{2L}}\,g(\eta),\ \ T=T_w=T_\infty+T_0\,e^{\frac{x}{2L}}\,\theta(\eta),\ \ C=C_w=C_\infty+C_0\,e^{\frac{x}{2L}}\,\varphi(\eta) \end{aligned}\right\} \tag{7}$$

Substitute equation (7) into equation (1-5) gives the non-linear ordinary differential equation (ODEs):

$$(1+\beta)f'''+ff''-2f'^2+\beta g'-2\left[M+\frac{1}{K}\right]f'+Gr\,\theta+Gc\,\varphi=0 \tag{8}$$

$$\left(1+\frac{\beta}{2}\right)g''-\beta(2g+f')+fg'-3gf'=0, \quad (9)$$

$$(1+R)\theta''+Pr\,(Nb\,\varphi'\theta'+Nt\,\theta'^2+f\theta'-f'\theta+H\theta)=0, \quad (10)$$

$$\varphi''+\frac{Nt}{Nb}\theta''+Le\,Pr\,(f\varphi'-Kr\,\varphi)=0, \quad (11)$$

The transformed boundary conditions are:

$$\left.\begin{array}{l} f'(0)=1,\ f(0)=S,\ \theta(0)=1, \quad Nb\,\varphi'(0)+Nt\,\theta'(0)=0, \\ g(0)=-nf''(0) \quad at\ y=0, \\ f'(\infty)\to 0,\theta(\infty)\to 0,\varphi(\infty)\to 0,g(\infty)\to 0 \quad as\ y\to\infty \end{array}\right\}, \quad (12)$$

Where η –similarity variable f, g, θ, and φ are dimensionless axial velocity, transfer velocity temperature, and nanoparticle concentration correspondingly, $\beta=\frac{k}{\mu}$ is micropolar parameter, $K=\frac{\upsilon L}{u_w k_1}$ Is the porosity parameter, $Nt=\frac{\tau D_T\,(T_w-T_\infty)}{\upsilon T_\infty}$ Is the thermophoresis parameter, $Nb=\frac{\tau D_B\,(C_\infty)}{\upsilon}$ Is the Brownian motion parameter, $Le=\frac{\alpha}{D_B}$ is Lewis number parameter $R=\frac{16\,\sigma\,{T_\infty}^3}{3kk^*}$ Is the radiation parameter, respectively. $M=\frac{2\sigma\,{B_0}^2\,L}{\rho_f\,u_w^2}$ Is the magnetic parameter, $Pr=\frac{\nu}{\alpha}$ is Prandtl number, $Gr=\frac{g\beta^+LT_0U_0}{u_w^3}$ Is the thermal Grashof number, $G=\frac{g\beta^-LC_0U_0}{u_w^3}$ is the solutal Grashof number, $H=\frac{2LQ}{\rho C_p\,u_w}$ Is the internal heat parameter, and $S=\frac{V_0}{\sqrt{\frac{\nu U_0}{2L}}}$ Is suction/injection parameter.

Pertinent physical factors

Here Cf_x, Nu_x, and Sh_x Illustrates the wall friction parameter, heat exchange rate, and mass diffusion rate respectively

$$\left.\begin{array}{l} Cf_x=\frac{2\tau_w}{\rho {U_w}^2}, \\ Nu_x=-\frac{Lq_w}{k(T_w-T_\infty)}, \\ Sh_x=\frac{Lj_w}{D_B(C_w-C_\infty)}, \end{array}\right\}, \quad (13)$$

Such as:

$$\left.\begin{array}{l} \tau_w=(\mu+k)\frac{\partial u}{\partial y}+kN. \\ q_w=-k\left(\frac{\partial T}{\partial y}\right), \\ j_w=-D_B\frac{\partial C}{\partial y} \end{array}\right\} at\ y=0\}, \quad (14)$$

Substitute equation (14) into (13) gives:

$$\left.\begin{array}{l} Cf_x\,{Re_x}^{0.5}=2(1+\alpha(1-n)f''(0), \\ Nu_x\,{Re_x}^{-0.5}=-\theta'(0), \\ Sh_x\,{Re_x}^{-0.5}=\varphi'(0). \end{array}\right\} \quad (15)$$

$Re_x=\frac{u_w\,x}{v_f}$ Is Reynolds's number.

Semi-Analytical Solution

The coupled differential equations (8) to (11) along with the boundary constraint (12) are solved through a semi-analytical approach called the Galerkin weighted residual scheme. This solution technique is employed due to its stability, consistency, and convergent, and it is applicable in solving linear and nonlinear differential equations, as demonstrated by [32-34]. For the solution procedures, basis functions are defined with the conferment of the Galerkin weighted residual scheme as follows:

$$\bar{f}(\eta)=a_0+a_1\eta+a_2\eta^2+\cdots+a_r\eta^r=\sum_{j=0}^{r}a_j\eta^r \quad (16)$$

$$\bar{g}(\eta)=b_0+b_1\eta+b_2\eta^2+\cdots+b_r\eta^r=\sum_{j=0}^{r}b_j\eta^r \quad (17)$$

$$\bar{\theta}(\eta)=c_0+c_1\eta+c_2\eta^2+\cdots+c_r\eta^r=\sum_{j=0}^{r}c_j\eta^r \quad (18)$$

$$\bar{\varphi}(\eta) = d_0 + d_1\eta + d_2\eta^2 + \cdots + d_r\eta^r = \sum_{j=0}^{r} d_j\eta^r \quad (19)$$

Apply the trial functions on the differential equations (8) to (12) to generate residual equations in vector form as $\bar{f}(\eta)$, $\bar{g}(\eta)$, $\bar{\theta}(\eta)$ and $\bar{\varphi}(\eta)$ to have

$$\boldsymbol{R_f} = (1+\beta)\bar{f}''' + \bar{f}\bar{f}'' - 2\bar{f}'^2 + \beta\bar{g}' - 2\left[M + \frac{1}{K}\right]\bar{f}' + Gr\bar{\theta} + Gc\,\bar{\varphi}, \quad (20)$$

$$\boldsymbol{R_g} = \left(1 + \frac{\beta}{2}\right)\bar{g}'' - \beta(2\bar{g} + f') + \bar{f}\bar{g}' - 3\,\bar{g}\,\bar{f}', \quad (21)$$

$$\boldsymbol{R_\theta} = (1+R)\bar{\theta}'' + Pr\left(Nb\,\varphi'\bar{\theta}' + Nt\,\bar{\theta}'^2 + \bar{f}\bar{\theta}' - \bar{f}'\bar{\theta} + H\bar{\theta}\right), \quad (22)$$

$$\boldsymbol{R_\varphi} = \bar{\varphi}'' + \frac{Nt}{Nb}\bar{\theta}'' + Le\,Pr\left(\bar{f}\bar{\varphi}' - Kr\,\bar{\varphi}\right), \quad (23)$$

The constant coefficients are determined by setting the residue to zero, this allows minimization of the residual error all over the fluid flow domain using the Galerkin integration method:

$$\boldsymbol{W_f} = \int R_{f(\eta)} a_r^f\, d\eta = 0,\ r = 0, 1, 2, \ldots, j \quad (24)$$

$$\boldsymbol{W_g} = \int R_{g(\eta)} b_r^g\, d\eta = 0,\ r = 0, 1, 2, \ldots, j \quad (25)$$

$$\boldsymbol{W_\theta} = \int R_{\theta(\eta)} c_r^\theta\, d\eta = 0,\ r = 0, 1, 2, \ldots, j \quad (26)$$

$$\boldsymbol{W_\varphi} = \int R_{\varphi(\eta)} d_r^\varphi\, d\eta = 0,\ r = 0, 1, 2, \ldots, j \quad (27)$$

Introduce the Galerkin integration technique into the residual equations over the dynamical fluid flow domain to determine the constant, thereby substituting the constant into the basic functions to obtain the solution for the equations.

$$\boldsymbol{R_f} = \int_0^\infty \left[(1+\beta)\bar{f}''' + \bar{f}\bar{f}'' - 2\bar{f}'^2 + \beta\bar{g}' - 2\left[M + \frac{1}{K}\right]\bar{f}' + Gr\bar{\theta} + Gc\,\bar{\varphi} = 0\right] d\eta, \quad (28)$$

$$\boldsymbol{R_g} = \int_0^\infty \left[\left(1 + \frac{\beta}{2}\right)\bar{g}'' - \beta(2\bar{g} + f') + \bar{f}\bar{g}' - 3\,\bar{g}\,\bar{f}' = 0\right] d\eta, \quad (29)$$

$$\boldsymbol{R_\theta} = \int_0^\infty \left[(1+R)\bar{\theta}'' + Pr\left(Nb\,\varphi'\bar{\theta}' + Nt\,\bar{\theta}'^2 + \bar{f}\bar{\theta}' - \bar{f}'\bar{\theta} + H\bar{\theta}\right) = 0\right] d\eta, \quad (30)$$

$$\boldsymbol{R_\varphi} = \int_0^\infty \left[\bar{\varphi}'' + \frac{Nt}{Nb}\bar{\theta}'' + Le\,Pr\left(\bar{f}\bar{\varphi}' - Kr\,\bar{\varphi}\right) = 0\right] d\eta, \quad (31)$$

The process of Galerkin weighted residual is repeated with varying parameter values, the solution procedures are executed in the Maple software environment for accuracy.

Results and Discussion

In this section, we thoroughly investigated the acquired results using graphs, as follows:

Fig.2 illustrates the impact of micropolar factor β on the axial velocity profile f'(η) at no wall porosity S=0 and wall porosity S=0.03, resulting in an improvement in the velocity rate. The improvement is due to lower flow resistance at the porous wall and enhanced microstructural effects caused by the micropolar factor (β). On the other hand side, the micropolar factor β on transfer velocity profile $g(\boldsymbol{\eta})$ at no wall porosity $S = 0$ and wall porosity $S = 0.03$ trends opposite in the velocity rate, the opposing trends of $g(\boldsymbol{\eta})$ with β Under S=0 and S=0.03 arise from the interplay between micro rotation effects, wall confinement, and momentum redistribution. At S=0, rotational effects suppress tangential transfer, while at S=0.03, the porous boundary facilitates the flow and enhances tangential velocity. This is presented in Fig.3

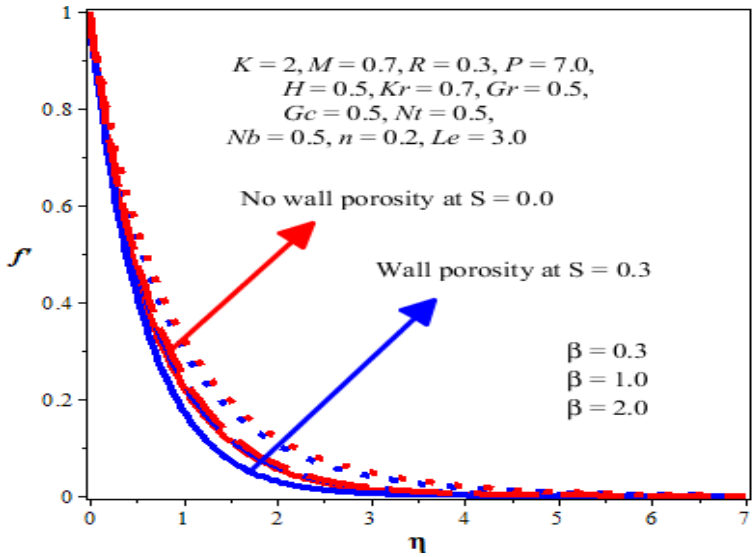

Fig. 2. Effect of β on dimensionless axial velocity

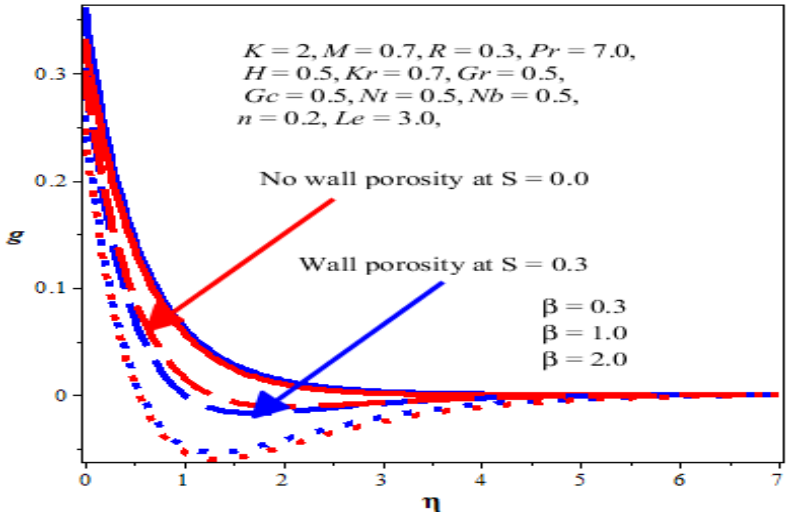

Fig. 3. Effect of β on dimensionless transfer velocity

Fig.4 illustrates the behavior of magnetic factor M on axial velocity profile $f'(\eta)$ at no wall porosity $S = 0$ and at wall porosity $S = 0.03$ it shows down in the velocity rate, this because, Meanwhile, there is an enhancement in axial velocity function when an increment shows in the values of thermal Grashof number Gr while low or high values of wall porosity the increase in axial velocity function $f(\eta)$ with higher Gr is due to the dominance of buoyancy forces that overcome viscous and micro rotation effects in micro polar fluids. Wall porosity modulates this effect by reducing flow resistance, leading to a more pronounced enhancement at higher porosity while still allowing for significant increases at low porosity. Highlight via Fig.5. Moreover, Fig.6 reveals that, when the radiation factor R improved to lead to the dimensionless temperature $\theta(\eta)$ increased, the increase in the dimensionless temperature $\theta(\eta)$with higher R is due to the stronger radiative heat transfer, which injects additional thermal energy into the system. This shifts the energy balance, raising the fluid's temperature rate, and vice versa the increment in the Prandtl Pr value led temperature function $\theta(\eta)$ down as seen the Graph .7, and the temperature rate $\theta(\eta)$ improve due to an increment of heat source parameter H The temperature rate $\theta(\eta)$ improves with an increased heat source parameter because of the additional thermal energy injected into the fluid system. This alters the energy balance in favor of higher temperatures, with the effect amplified by conduction and microstructural dynamics in micro polar fluids observed in Fig .8

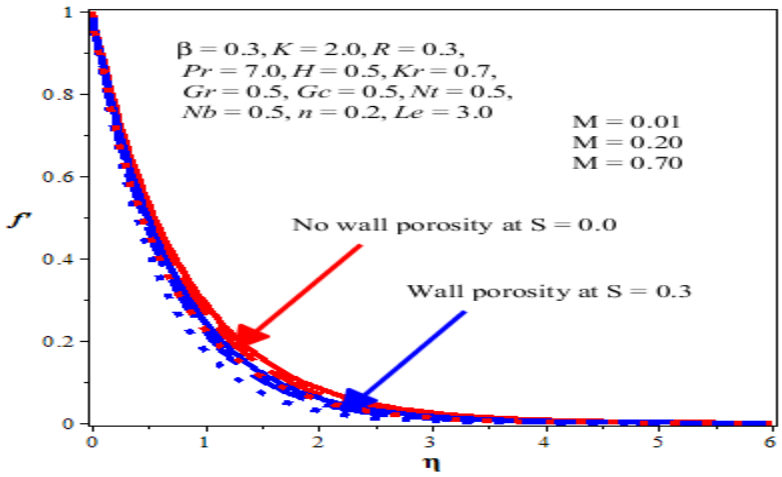

Fig. 4. Effect of M on dimensionless axial velocity

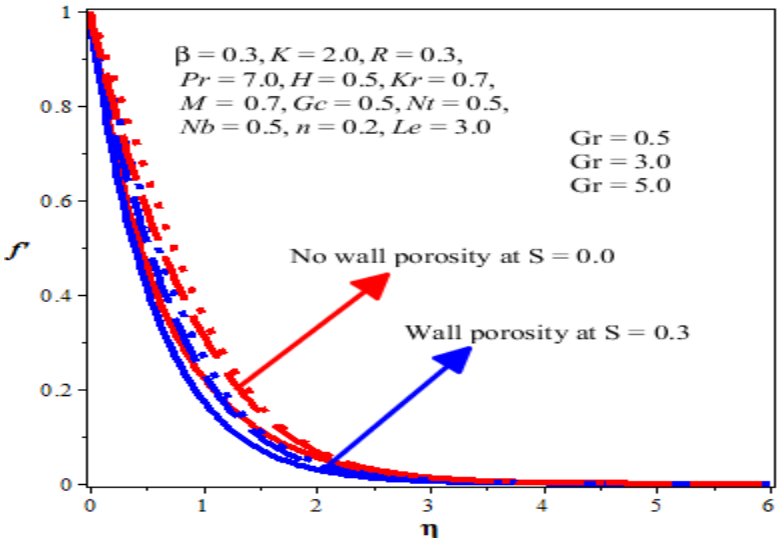

Fig. 5. Effect of Gr on dimensionless axial velocity

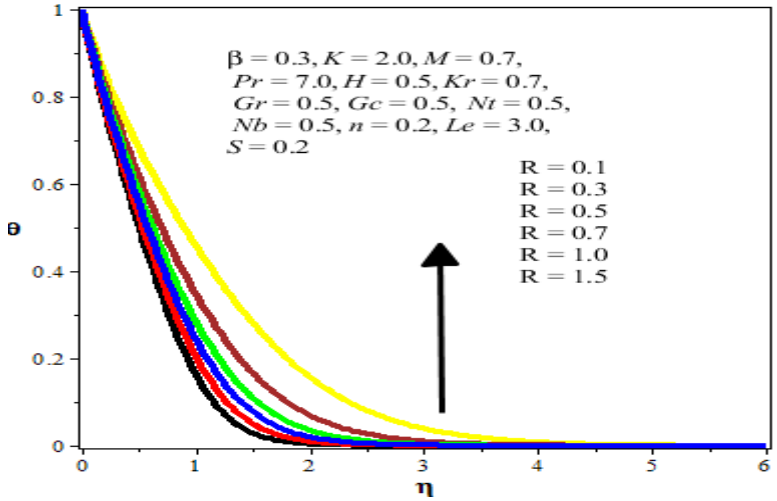

Fig. 6. Effect of R on dimensionless temperature

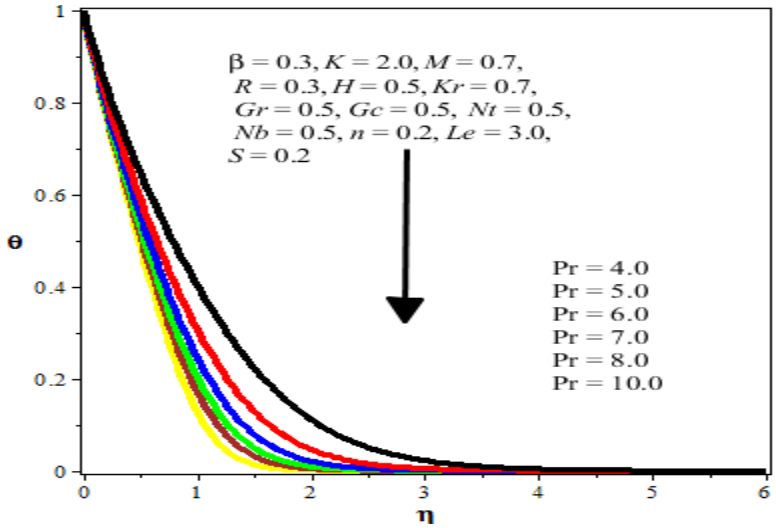

Fig. 7. Effect of Pr on dimensionless temperature

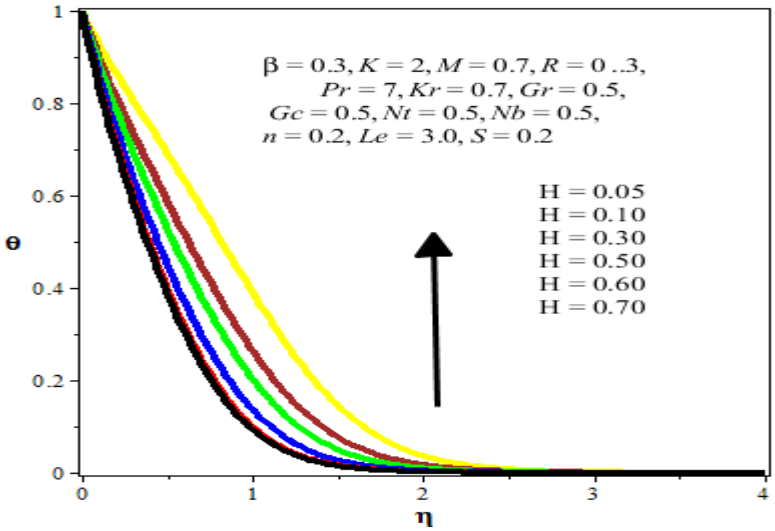

Fig. 8. Effect of H on dimensionless temperature

Fig .9, and Fig .10 Elucidate the behavior of thermophoresis parameter Nt on dimensionless temperature $\theta(\boldsymbol{\eta})$ and concentration factor $\varphi(\boldsymbol{\eta})$ both are growth because the thermophoresis parameter causes growth in both the dimensionless temperature $\theta(\boldsymbol{\eta})$ and concentration $\varphi(\boldsymbol{\eta})$ because it strengthens the particle migration from hotter to cooler regions. This migration not only enhances thermal energy transfer but also increases particle accumulation, leading to simultaneous increases in thermal and concentration fields, in Fig .11 when the Brownian motion parameter Nb increases, the concentration rate behaves negatively, the negative behavior of the concentration rate $\varphi(\boldsymbol{\eta})$ with increasing arises from the enhanced random diffusion of particles due to stronger Brownian motion Nb This leads to particle dispersion away from high-concentration regions, reducing the overall concentration near boundaries and within localized zones. As well as at increased the values of Lewis Le number in Fig .12 also decreases, and graph.13. Explains that, the concentration $\varphi(\boldsymbol{\eta})$ decreases with an increase in the chemical reaction Kr parameter because a stronger reaction rate leads to faster consumption of the species. This depletion outpaces replenishment by diffusion or convection, resulting in a net reduction in $\varphi(\boldsymbol{\eta})$throughout the fluid domain

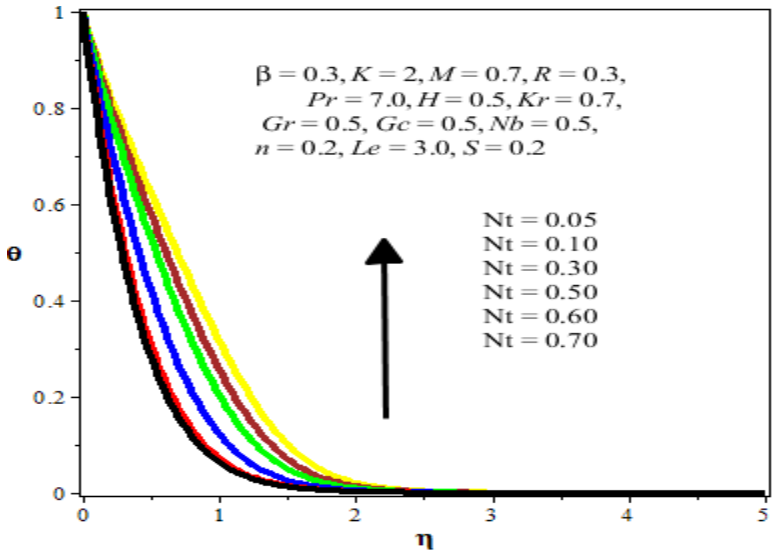

Fig. 9. Effect of Nt on dimensionless temperature

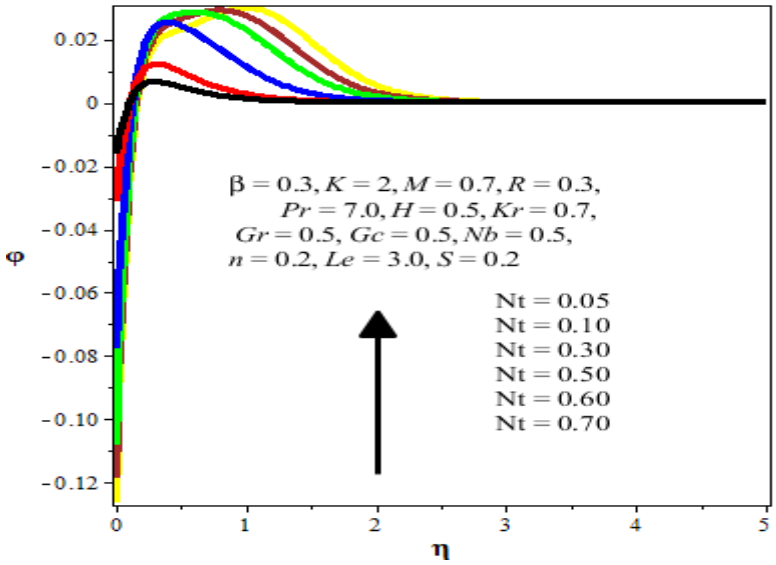

Fig. 10. Effect of Nt on dimensionless concentration

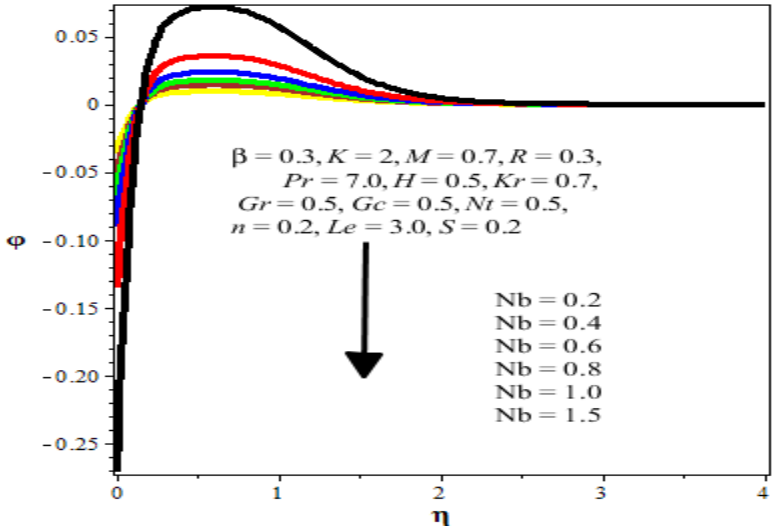

Fig. 11. Effect of Nb on dimensionless concentration

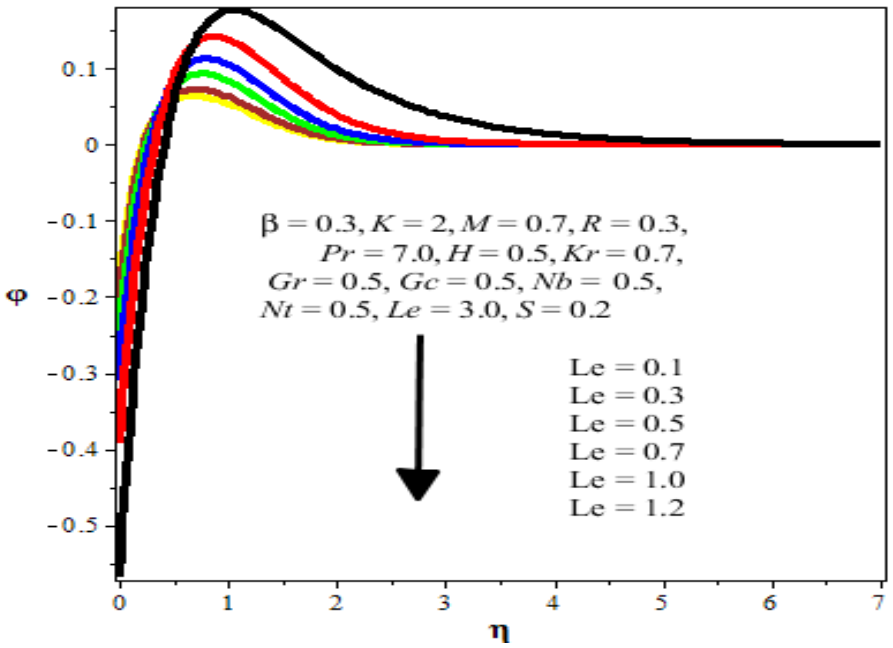

Fig. 12. Effect of Le on dimensionless concentration

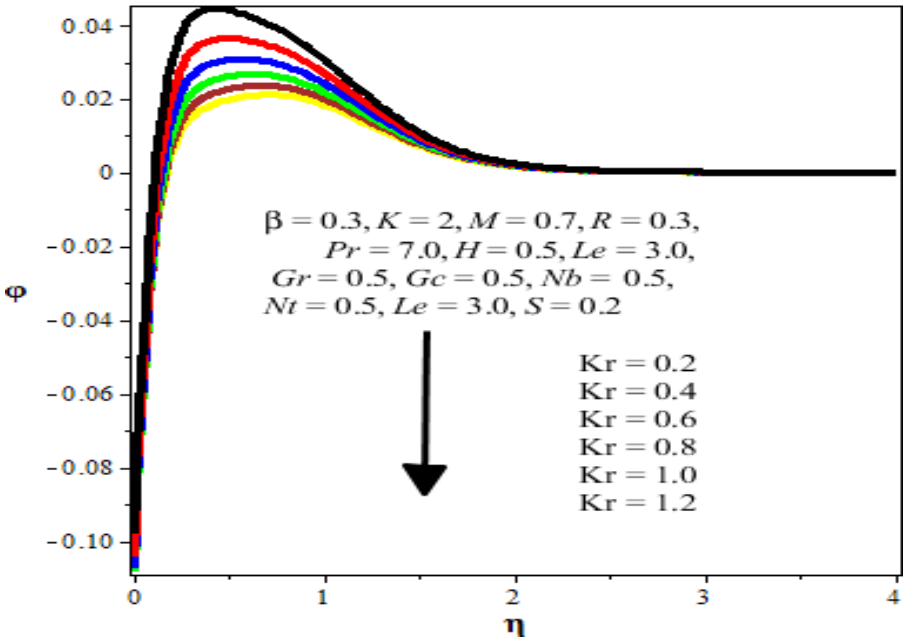

Fig. 13. Effect of Kr on dimensionless concentration

Table 1. Comparison of $-\theta'(0)$ for different values of the Prandtl number

R	K	Ishak [35]	Puneet Rana et.al	Present values
2	0	0.3547	[36]	0.3570743
	1	0.3893	0.357185	0.3884078
	2	0.4115	0.385299	0.4108294
2	0	0.2588	0.410053	0.2595098
	1	0.2895	0.259925	0.2958247
	2	0.3099	0.297511	0.3087623
			0.310974	

Table 2. Effect of pertinent parameters on physical interest quantities

M	S	R	K	$C_f Re_x^{0.5}$	$N_{UX} Re_x^{-0.5}$	$Sh_x\ Re_x^{-0.5}$
0.1	0.5	2.0	0.9	-1. 878316	-1.199482	1.199482
0.3				-1.965403	-1.172608	1.172608
0.5				-2.048607	-1.145959	1.145959
0.7				-2.128398	-1.110399	1.110399
0.9				-2.205253	-1.092805	1.092805
0.4	0.1	2.0	0.9	-1.794271	-0.415097	0.415097
	0.5			-2.007459	-1.159264	1.159264
	1.0			-2.260623	-1.827707	1.827707
	1.5			-2.526958	-2.489211	2.489211
	2.0			-2.808434	-3.163002	3.163002
0.4	0.5	0.5	0.9	-2.034312	-1.713713	1.713713
		1.0		-2.025072	-1.490912	1.490912
		1.5		-2.016071	-1.310647	1.310647
		2.0		-2.007459	-1.159264	1.159264
		2.5		-1.999489	-1.031116	1.031116
0.4	0.5	2.0	0.3	-2.775254	-0.842487	0.842487
			0.5	-2.346847	-1.040537	1.040537
			0.7	-2.135214	-1.117081	1.117081
			1.0	-1.969672	-1.174094	1.174094
			1.5	-1.812682	-1.219113	1.219113

Conclusion:

This research looks at the radioactive mixed convection flow of a micro polar nan fluid over an exponentially permeable stretched sheet, which produces internal heat. The governing partial differential equations (PDEs) are converted into nonlinear ordinary differential equations (ODEs) via similarity transformations. These ODEs are solved with the semi-analytical Galerkin weighted residual method. The Galerkin technique is employed iteratively to determine various parameter values, with all computations carried out in the Maple software environment to ensure accuracy. The results are presented in graphs and tables, demonstrating the effects of various fluid parameters. Statistics show that these features have a considerable impact on flow properties, as well as heat and mass transfer rates. The findings are described below, as follows;

1. The axial velocity function improves with rising Gr and β values but decreases with increasing M values.
2. The transfer velocity rate decreases with increasing β values.
3. The dimensionless temperature increased when the values of $R, Nt, and\ H$ grew while reducing when the values of Pr increased.
4. The dimensionless concentration increased when Nt values increased, but decreased while Kr $Kr, Le, and\ Nb$ values increased.

This research investigation helps to understand and optimize the behavior of complex systems with significant microstructural and rotational impacts. Their uses are many, ranging from healthcare to energy, industry, and environmental engineering, making them essential components of modern scientific and industrial achievements.

References:

[1] S. Choi, Enhancing thermal conductivity of fluid with nanoparticles, ASME-Publ. Fed, 231 (1995) 99-106.

[2] B.Ganga, SMY Ansari, NV .Ganesh, AKA. Hakeem. MHD flow of Buongiorno model nanofluid over a vertical plate with internal heat generation/absorption. Prop Pow Res. 2016; 5 (3): 211-222.

[3] AKA. Hakeem, B. Ganga , SMY. Ansari, NV. Ganesh . Analytical and numerical studies on hydromagnetic flow of Buongiorno model nanofluid over a vertical plate. J Heat Mass Transf Res. 2016; 3(2): 153-164.
[4] AKA. Hakeem, M. Govindaraju, B. Ganga. influence of inclined Lorentz forces on entropy generation analysis for viscoelastic fluid over a stretching sheet with nonlinear thermal radiation and heat source/sink. J Heat Mass Transf Res. 2019; 6(1):1-10.
[5] I.Khan , T.Chinyoka ,EAA. Ismail, FA. Awwad, Z. Ahmad. MHD flow of third-grade fluid through a vertical micro-channel filled with porous media using semi-implicit finite difference method. Alex Eng J. 2024; 86:513-524.
[6] F.Hasin , Z..Ahmad , F. Ali, N. Khan , I.Khan , SM.Eldin . Impact of nanoparticles on vegetable oil as a cutting fluid with fractional ramped analysis. Sci Rep. 2023; 13: 7140.
https://doi.org/10.1038/s41598-023-34344-z
[7] N. Khan , F. Ali, Z. Ahmad , S.Murtaza , AH. Ganie,I. Khan , Eldin SM. A time fractional model of a Maxwell nanofluid through a channel flow with applications in grease, Sci Rep. 2023; 13: 4428. https://doi.org/10.1038/s41598-023-31567-y.
[8] A.Noghrehabadi, R. Pourrajab, M.Ghalambaz. Effect of partial slip boundary condition on the flow and heat transfer of nanofluids past stretching sheet prescribed constant wall temperature. Int J Therm Sci. 2012; 54; 253-250.
[9]WA. Khan, I. Pop. Boundary layer flow of a nanofluid past stretching sheet. Int J Heat Mass Transf. 2010; 53: 2477-2483.
[10] S. Nadeem, RU .Haq, NS .Akbar, C. Lee, ZH. Khan. Numerical study of boundary layer flow and heat transfer of Oldroyd-B nanofluid towards a stretching sheet. PLoS One. 2013; 6: e69811. https://doi.org/10.1371/journal.pone.0069811
[11] OD. Makinde,WA. Khan,ZH. Khan . Buoyancy effects on MHD stagnation point flow and heat transfer of nanofluid past a convectively heated stretching/shrinking sheet. Int J Heat Mass Transf. 2013; 62: 526-533.
[12].AC. Eringen. Theory of micropolar fluids. J Math Mech. 1966; 16:1-18.
[13] AC. Eringen. Theory of thermo micropolar fluids. J Math Appl. 1972; 38:480-495.
[14] T. Ariman, MA .Turk, Sylvester ND. Application of microrotation fluid mechanics review. Int J Sci. 1974; 11:905-930.
[15] T.Ariman , MA.Turk, Sylvester ND. Application of microrotation fluid mechanics. Int J Sci. 1974; 12:273-293.
[16] G.Lukaszewicz Micropolar fluids: theory and Application. Birkhauser. Basel. 1999.
[17] Eringen AC. Microcontinuum fluid theories II: fluent media. Springer New York, 2001.
[18] T.Oreyeni, K. Ramesh, MK.Nayak, PA. Oladele . Triple stratification impacts on an inclined hydromagnetic bioconvective flow of micropolar nanofluid with exponential space-based heat generation. Waves in random and complex media. 2022.
https://doi.org/10.1080/17455030.2022.2112994
[19] OK. Koriko, AJ. Omowaye, AO. Popoola,T. Oreyeni , AA.Adegbite , EA .Oni, E. Omokhuale, MM. Altine. Insight into dynamics of hydromagnetic flow of micropolar fluid containing nanoparticles and gyrotactic microorganisms at weak and strong concentrations of microelements: Homotopy Analysis Method. Amer J Comput Math. 2022; 12:267-282. https://doi.org/10.4236/ajcm.2022.122017
[20] OK. Koriko, IL. Animasaun, AJ. Omowaye, T..Oreyeni. The combined influence of nonlinear thermal radiation and thermal stratification on the dynamics of micropolar fluid along a vertical surface. Multidisc Mod Mat Struc. 2018; 15(1): 133-155.
https://doi.org/10.1108/MMMS-12-2017-0155
[21] G. Ahmadi, Self-similar solution of incompressible micropolar boundary layer flow over semi-infinite flat plate. Int J Eng Sci. 1976; 14:639-646.
[22] KA.Kline .Aspin-vorticity relation for unidirectional plane flows of micropolar fluids. Int J Eng Sci. 1977; 15:131-134.

[23] Pedersen J, Mcnitt RP. Boundary layer theory for micropolar fluids. Recent Adv Eng Sci. 1970; 5: 405-476.
[24] Mazhar Hussain., Shereen Fatima, Mubashir Qayyum, Radiative mixed convection flow of Casson nanofluid through exponentially permeable stretching sheet with internal heat generation, Journal of Mathematics (2024)
[25] O. Ibukun, M. Sabyasachi, P. Sibanda, Unsteady Casson Nanofluid flow over a stretching sheet with thermal radiation, convective and slip boundary conditions, Alexandria Eng. J. (2016) 55, 1025-1035.
[26] J. Buongiorno, Convective transport in nanofluids, J. Heat Trans, 128 (2006) 2040-250.
[27] A. Noghrehabadi, R. Pourrajab, M. Ghalambaz, Effect of partial slip boundary condition on the flow and heat transfer of nanofluids past stretching sheet prescribed constant wall temperature, Int. J. Ther. Sci.54 (2012) 253-261.
[28] W. A. Khan, I. Pop, Boundary layer flow of a nanofluid past stretching sheet, Int. J. Heat Mass Trans, 53 (2010) 2477-2483.
[29] S. Nadeem, R.U. Haq, N.S Akbar, C. Lee, Z. H. Khan, Numerical study of boundary layer flow and heat transfer of Oldoroyd-B nanofluid towards a stretching sheet, PLoS One 8 (2013) e6981.
[30] O. D. Makinde, W. A. Khan, Z.H. Khan, Boundary effects on MHD stagnation point and heat transfer of a nanofluid past convective heated stretching/shrinking sheet, Int.J. Heat Mass Trans. 62 (2013) 526-533.
[31] N. A. Haroun, P. Sibanda, S. Modal, S.S. Motsa, On unsteady MHD mixed convection in a nanofluid due to stretching/shrinking surface with suction/injection using spectral relaxation method, Bound, Vale, Problems. 1 (2015) 1-17.
[32] A.D. Ohaegbue, S.O. Salawu, R.A. Oderinu, A.A. Oyewumi, A.O. Akindele, J.A. Owolabi, Thermal criticality and two-step diffusion-reaction of electromagnetic Casson-Williamson fluid flow along a vertical channel with convective cooling under bimolecular kinetic. Chemical Physics, 587 (2024) 112411.
[33] S.O. Salawu, A.M. Obalalu, E.O. Fatunmbi, A.B. Disu, Tiny particles thermal motile in magnetized chemically reacting upper-convective Maxwell stagnation point fluid with radiation. Results in Engineering, 23 (2024) 102593.
[34] S.O. Salawu, E.O. Fatunmbi, R.A. Kareem, O.M. Akinmoladun, S.D. Ogundiran, Radiating and Joule heating on heat and mass transfer of magnetized tiny particles in tangent hyperbolic nonlinear porosity flow with Riga plate and Arrhenius reaction. Partial Differential Equations in Applied Mathematics, 11 (2024) 100840.
[35] S. Pramanik, “Casson fuid fow and heat transfer past an exponentially porous stretching surface in presence of thermal radiation,” Ain Shams Engineering Journal, vol. 5, no. 1, pp. 205–212, 2014.
[36] P Rana, R.Dhanai,. &, L. Kumar. Mhd slip flow and heat transfer of al2o3-water nanofluid over a horizontal shrinkingcylinder using buongiorno’s model: Effect of nanolayer and nanoparticle diameter. Adv. Powder Technol. 28, 1727–1738(2017)
[37] Fakhraldeen Gamar, MD. Shamshuddin, M. Sunder Ram, S. O. Salawu & E. O.Fatunmbi, Exploration of thermal radiation and stagnationpoint in MHD micropolar nanofluid flow over astretching sheet with Navier slip, Numerical Heat Transfer, Part A: Applications An Int. J. of Computation and Methodology, DOI: 10.1080/10407782.2024.2338264